Service Availability Oriented *p*-Cycle Protection Design in Elastic Optical Networks

Xiaoliang Chen, Fan Ji, and Zuqing Zhu

***Abstract*—In this paper, we develop a theoretical model to precisely analyze the service availability of networks with preconfigured cycles (*p*-cycles). By considering the dependence among protection domains and all the scenarios when a lightpath is available, our model can estimate the service availability more precisely than those in previous work. Then, based on the availability analysis, we propose a service availability oriented *p*-cycle configuration algorithm for dynamic elastic optical networks (EONs), namely, the number of relevant links (NRL)-based *p*-cycle design algorithm (NRL-*p*-cycle). The simulations compare the proposed algorithm with two benchmark *p*-cycle design algorithms that are based on the protection efficiency of *p*-cycles. Simulation results show that the proposed algorithm can effectively improve the service availability in EONs while keeping the blocking probability almost unchanged.**

***Index Terms*—Elastic optical networks (EONs); Lightpath service availability; Preconfigured cycle (*p*-cycle).**

I. Introduction

Recently, spectrum-sliced elastic optical networks (EONs) have attracted intensive research interest because of their high bandwidth efficiency and flexible spectrum management in the optical layer [1]. By leveraging advanced transmission technologies, such as optical orthogonal frequency-division multiplexing (O-OFDM), lightpaths in EONs transmit data using bandwidth-variable transponders. each of which operates on a series of spectrally contiguous frequency slots (FSs). Therefore, EONs can allocate bandwidth with fine granularity, such as 6.25 or 12.5 GHz, and potentially provide a better solution for the integration of physical transmission and upper-layer applications than traditional fixed-grid wavelength-division multiplexing (WDM) networks [1].

Meanwhile, network survivability has been and will always be an important problem to investigate for optical networks. It is known that, in optical networks, the amount of traffic disruption and data loss caused by failures of network components would be huge; for instance, a single optical fiber can carry over 20 Tb/s live traffic [2]. Therefore, it is not only important but also necessary to investigate service protection schemes for EONs. On the other hand, in practical network operation, service providers usually ensure differentiated quality of service (QoS) by specifying the targets of service availability in the service-level agreements (SLAs) [3]. Here, the service availability of a lightpath request is defined as

$$A = \frac{T - T_{\text{off}}}{T}, \tag{1}$$

where T is the total provisioning time and T_{off} is the duration of the service outage due to link failures in the network [4]. Statistically, service availability is just the probability that a lightpath's service is available at any time point. Since SLA violations will cause huge capital loss to service providers, we need to evaluate the service availability for protection schemes and study service-availability-oriented protection design to ensure SLAs in EONs.

Previous studies have investigated protection design in EONs from the perspective of path protection. In [5], by assuming that the protection path could consume less bandwidth than the working one, Sone *et al.* proposed a bandwidth squeezed restoration scheme for dedicated path protection (DPP) in EONs. The shared path protection (SPP) scheme was investigated in [6] for improving the spectral efficiency of protection design in EONs, and a heuristic based on K-shortest path routing and first-fit spectrum assignment was proposed. The authors of [7] proposed a single-path provisioning and multi-path recovery scheme. They considered both the DPP and SPP schemes, and formulated mixed integer linear programming (MILP) models to optimize the protection design. In [8], Klinkowski and Walkowiak studied the problem of static routing and spectrum assignment (RSA) in EONs with DPP, developed an integer linear programming (ILP) model, and proposed a heuristic based on adaptive frequency assignment. The problem of static RSA for translucent EONs with SPP was studied in [9], and both an ILP model and a heuristic were developed. An experimental demonstration of adaptive quality-of-transmission (QoT) degradation restoration with DPP in EONs was discussed in [10]. In [11], Liu *et al.* proposed an SPP scheme for EONs, which was named "elastic separate-protection-at-connection" and facilitated spectrum sharing between

Manuscript received May 19, 2014; revised July 28, 2014; accepted September 3, 2014; published September 25, 2014 (Doc. ID 211800).

The authors are with the School of Information Science and Technology, University of Science and Technology of China, Hefei, Anhui 230027, China (e-mail: zqzhu@ieee.org).

http://dx.doi.org/10.1364/JOCN.6.000901

the working and backup traffic. A survivable multipath provisioning scheme was presented in [12], and the authors developed an ILP model and a heuristic to solve the static survivable multipath RSA problem.

Although the aforementioned SPP schemes are straightforward to implement and can provide high protection efficiency, they may result in relatively long restoration time because the backup resources can only be reserved but not preconfigured. When a link failure happens, we need to reconfigure all the nodes along the working and backup paths for restoration [13]. Alternatively, link-based preconfigured cycle (p-cycle) protection was proposed in [14]. For this type of protection scheme, a p-cycle is preconfigured to protect a working link, and, when that link fails, the p-cycle is activated for restoration. Since we need to reconfigure only the two end nodes of the failed link for restoration, the restoration time is relatively short. Moreover, a p-cycle can protect not only the links that are on-cycle but also those that straddle it. Due to these advantages, p-cycle-based protection schemes have been studied intensively for fixed-grid WDM networks [15–19]. However, implementations of p-cycle schemes in EONs are still underexplored, and only a few works in this area have been reported [20].

The service availability of networks with p-cycles was theoretically analyzed in [21–24], where the authors first tried to enumerate all the dual-link-failure scenarios that would cause a service outage on a lightpath, and then calculated their probabilities to estimate the lightpath's service unavailability. However, this type of approach did not consider the cases in which there are more than two failed links, and this can make the estimation inaccurate. For a lightpath that is protected by multiple p-cycles, the studies partition the network topology into several domains, each of which contains a few working links and the p-cycle that protects them. Then, they derive the lightpath's service availability with the availability of each domain under the assumption that the operations of the domains are independent. However, as we will show later in this paper, this assumption may not be valid for certain cases and can cause noticeable estimation errors.

In this paper, we first improve the theoretical models in [21–24] to consider the failure scenarios in which there are more than two failed links and treat the multiple-p-cycle scheme in a nonindependent manner, and then formulate a precise model to estimate the service availability of networks with p-cycles. Based on the availability analysis, we develop a dynamic p-cycle design algorithm for EONs that can effectively improve the service availability of dynamic provisioning in EONs. The contributions of the paper can be summarized as follows:

- We develop a novel theoretical model that checks the multiple link-failure scenarios in which a lightpath's service is still available, and consider the failure scenarios in a nonindependent manner to precisely estimate the service availability for lightpaths in networks with p-cycle protection.
- With the theoretical model, we study service-availability-oriented lightpath provisioning with p-cycle design in dynamic EONs and propose a heuristic to improve the service availability efficiently. To the best of our knowledge, this is the first work to address service-availability-oriented lightpath provisioning in dynamic EONs.

The rest of the paper is organized as follows. Section II presents the theoretical model for analyzing the service availability of networks with p-cycles. The service-availability-oriented p-cycle design for dynamic EONs is described in Section III, and the performance evaluation is discussed in Section IV. Finally, Section V summarizes the paper.

II. Theoretical Analysis on Service Availability in Networks With p-Cycles

In this section, we provide theoretical analysis on the service availability in networks with p-cycles. The network topology is modeled as a graph $G(V, E)$, where V and E represent the sets of the nodes and directed links in it, respectively. Similar to previous studies [21–24], we consider only link failures and assume that each link $e \in E$ associates with an availability a_e. A lightpath from source node s to destination node d $(s, d \in V)$ uses the routing path $\mathcal{R}_{s,d}$, which contains all the traversing links. To ensure 100% restoration against single link failures, we design a set of p-cycles $\mathbb{C}_{\mathcal{R}_{s,d}}$ to protect each link on the path. Also, similar to previous work [22], we assume that all the p-cycles can be shared among working links, and they are fully loaded, which means that they reach the maximum protection capabilities. With this model, we analyze the service availability of the lightpath when more than one link fails in the network.

A. Single-p-Cycle Case

We first consider the simplest case, in which the whole routing path of a lightpath $\mathcal{R}_{s,d}$ is protected by one p-cycle $\mathcal{C}_{\mathcal{R}_{s,d}}$. Figure 1(a) shows an illustrative example for this case. In Fig. 1(a), working path $1 \to 2 \to 5$ is protected by the p-cycle $1 \to 6 \to 5 \to 4 \to 3 \to 2 \to 1$. The restoration segments for Links $1 \to 2$ and $2 \to 5$ are depicted with dashed lines, i.e., $1 \to 6 \to 5 \to 4 \to 3 \to 2$ and $2 \to 1 \to 6 \to 5$, respectively. Here, we refer to the links that a p-cycle traverses from the opposite direction as its on-cycle links, for instance, Links $1 \to 2$ and $5 \to 6$ in Fig. 1(a). We refer to the links that straddle a p-cycle as its straddling links, e.g., Links $2 \to 5$ and $5 \to 2$ in Fig. 1(a).

To analyze the service availability for this case, we define the following notation:

- ρ: availability of each link, which is assumed to be the same for all the links, i.e., $a_e = \rho$, $\forall\, e \in E$.
- H_o: number of links on $\mathcal{R}_{s,d}$ that are on-cycle links of the p-cycle $\mathcal{C}_{\mathcal{R}_{s,d}}$.
- H_s: number of links on $\mathcal{R}_{s,d}$ that are straddling links of the p-cycle $\mathcal{C}_{\mathcal{R}_{s,d}}$.

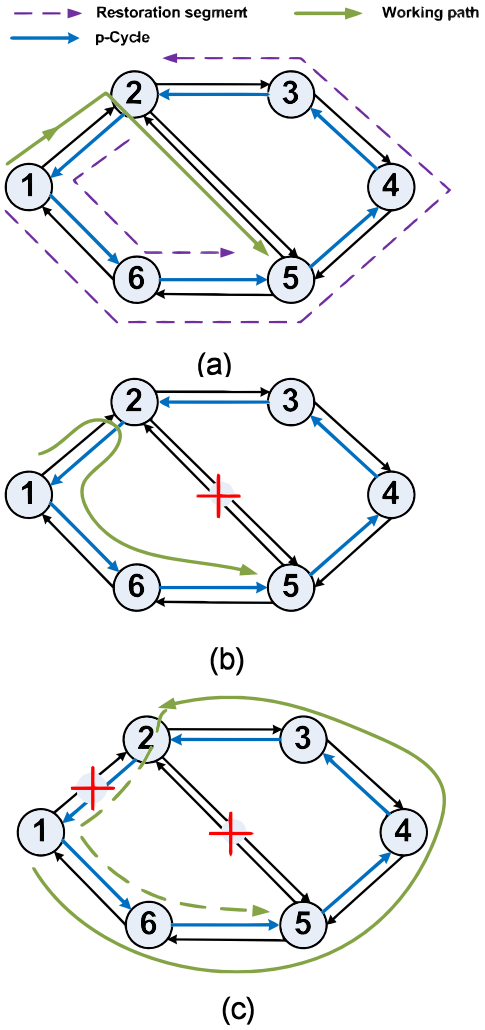

Fig. 1. Example of the single-p-cycle case: (a) working path, p-cycle, and the restoration segments of working links, (b) single working link failure, and (c) dual working link failures.

- H: total number of links on $\mathcal{R}_{s,d}$.
- L: total number of links on $\mathcal{C}_{\mathcal{R}_{s,d}}$.
- L_s: half-number of links in $G(V,E)$ that straddle $\mathcal{C}_{\mathcal{R}_{s,d}}$.
- L_e: number of links on $\mathcal{C}_{\mathcal{R}_{s,d}}$ that are used to protect a link $e \in \mathcal{R}_{s,d}$.

We treat all the working links with the same priority, and, thus, in network operation, a link that fails early is restored early. Then, a lightpath's service is available when and only when one of the following conditions is true.

Condition 1: None of its working links fail.

Condition 2: Along its routing path, only one working link fails, and the corresponding restoration segment is not used to recover other previously failed working link(s).

If there are multiple working link failures, the lightpath's service can be disrupted. Here, we assume that a link failure (i.e., fiber cut) between two nodes causes service outages in both directions. For instance, in Fig. 1(b), if there is a link failure between Nodes 2 and 5, both Link $2 \to 5$ and Link $5 \to 2$ become unavailable. In Fig. 1(c), when Links $1 \to 2$ and $2 \to 5$ both fail, the restoration segment $1 \to 6 \to 5 \to 4 \to 3 \to 2$ is activated to recover the service on Link $1 \to 2$ and then the network tries to activate the restoration segment $2 \to 1 \to 6 \to 5$ and recover the service on Link $2 \to 5$. However, since $2 \to 1 \to 6 \to 5$ traverses the failed link $2 \to 1$, the service on Link $2 \to 5$ cannot be restored. Note that, according to the working principle of p-cycles, the network cannot select segment $1 \to 6 \to 5$ on the p-cycle to restore the lightpath, as p-cycle is a link-based protection scheme and the restoration involves only the two end nodes of the failed link. In other words, p-cycle preconfigures a protection cycle for each working link and during a link failure, the two end nodes of the failed link switch the traffic on it to the cycle locally to realize fast restoration. As everything is preconfigured and the rerouting process is not involved, switching the lightpath in Fig. 1(c) from $1 \to 2 \to 5$ to $1 \to 6 \to 5$ for restoration is not feasible for p-cycle.

The service availability of the lightpath can be obtained by considering the following three scenarios, in which the service on it is still available even when there are multiple link failures. Here, we assume that, when multiple links fail simultaneously, the failed working links that share the same p-cycle have equal probability to be restored successfully [22].

Scenario 1: None of the working links on its routing path $\mathcal{R}_{s,d}$ fail, and the probability for this scenario to happen is

$$A_1 = \rho^H. \tag{2}$$

Scenario 2: Only one on-cycle working link fails and the required resources on the p-cycle have not been used for restoring the working links of other lightpaths. The probability for this scenario to happen is

$$A_2 = H_o(1-\rho)\rho^{H_s+L-1} \sum_{k=0}^{L_s-H_s} \frac{1}{1+k} \binom{L_s-H_s}{k} \rho^{L_s-H_s-k}(1-\rho)^k, \tag{3}$$

where the term $(1-\rho)\rho^{H_s+L-1}$ represents the case when one of the on-cycle working links fails while all the straddling working links and other on-cycle links are working, and the summation term enumerates all the nonworking straddling link failures that may compete with the failed working link for the backup resources. Let $N_s = L_s - H_s$ and $q = 1-\rho$, and we obtain

$$\begin{aligned} &\sum_{k=0}^{N_s} \frac{1}{k+1} \binom{N_s}{k} \rho^{N_s-k} q^k \\ &= \frac{1}{q(N_s+1)} \sum_{k=0}^{N_s} \binom{N_s+1}{k+1} \rho^{N_s-k} q^{k+1} \\ &= \frac{1-\rho^{N_s+1}}{q(N_s+1)}. \end{aligned} \tag{4}$$

By combining Eqs. (3) and (4), we have

$$A_2 = \frac{H_o(1-\rho^{L_s-H_s+1})}{L_s-H_s+1}\rho^{H_s+L-1}. \tag{5}$$

Scenario 3: Only one straddling working link fails and the required resources on the p-cycle have not been used for restoring the working links of other lightpaths. The probability for this scenario to happen is

$$A_3 = \sum_{i=1}^{H_s}(1-\rho)\rho^{H_s-1}\rho^{L_e}\Bigg[\rho^{L-L_e}\sum_{k=0}^{L_s-H_s}\frac{1}{k+1}\binom{L_s-H_s}{k} \times \rho^{L_s-H_s-k}(1-\rho)^k + \binom{L-L_e}{1}\rho^{L-L_e-1}(1-\rho) \times \sum_{k=0}^{L_s-H_s}\frac{1}{k+2}\binom{L_s-H_s}{k}\rho^{L_s-H_s-k}(1-\rho)^k\Bigg]. \tag{6}$$

Here, $(1-\rho)\rho^{H_s-1}\rho^{L_e}$ represents the case where only one straddling working link fails and its protection segment is working, while the terms in $[\cdot]$ enumerate all the failures on the nonworking straddling links and on-cycle ones, which may compete with the failed working link for the backup resources. By combining Eqs. (4) and (6), we have

$$A_3 = \sum_{i=1}^{H_s}\rho^{H_s+L_e-1}\Bigg[\rho^{L-L_e}\frac{1-\rho^{L_s-H_s+1}}{(L_s-H_s+1)} + (L-L_e) \times \rho^{L-L_e-1}\Bigg(\frac{1-\rho^{L_s-H_s+2}-(L_s-H_s+2)\rho^{L_s-H_s+1}(1-\rho)}{(L_s-H_s+1)(L_s-H_s+2)} + \frac{(1-\rho^{L_s-H_s+1})(1-\rho)}{L_s-H_s+1}\Bigg)\Bigg]. \tag{7}$$

Since Scenarios 1–3 are independent, we can obtain the service availability of the single-p-cycle case as

$$A = A_1 + A_2 + A_3. \tag{8}$$

B. Dual-p-Cycle Case

Figure 2(a) illustrates an example in which the lightpath $1 \to 5 \to 3 \to 6$ is protected by two p-cycles, $1 \to 2 \to 3 \to 4 \to 5 \to 1$ and $3 \to 5 \to 7 \to 6 \to 3$. We define a protection domain as a p-cycle together with the links it protects [22]. For instance, Fig. 2(b) shows that the lightpath and the two p-cycles can be divided into two protection domains. For this case, when analyzing a lightpath's service availability, previous works [21–24] assumed that the protection domains are independent. However, this assumption may be invalid for some cases. For example, in Fig. 2(b), a link-failure on Link $3 \to 5$ can affect both domains, and, therefore, the two domains are not independent. In this subsection, we try to avoid the inaccuracy on service availability caused by this assumption. The service availability of the lightpath can also be obtained by considering the

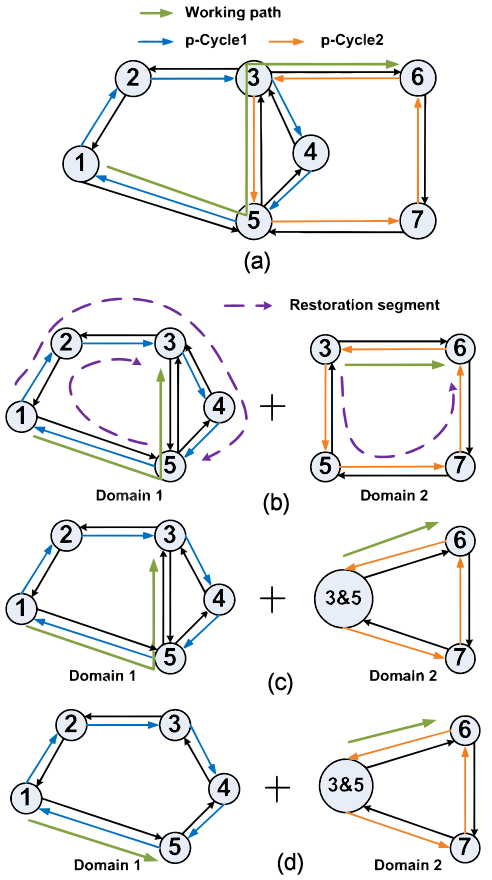

Fig. 2. Example for the dual-p-cycle case: (a) working path and p-cycle, (b) protection domains, (c) topology changes for Scenario 2, and (d) topology changes for Scenario 3.

following three scenarios. For the analysis, we define several additional notations:

- $H_{i,j}$: number of working links that belong to domain i $(i = 1, 2)$, in Scenario j $(j = 1, 2, 3)$.
- $A_{i,j}^{(d)}$: availability of domain i in Scenario j.
- L_c: number of common links of the two domains.

Scenario 1: None of the links on the lightpath's working path fail, and the probability for this scenario to happen is

$$A_1 = \rho^{H_{1,1}+H_{2,1}}. \tag{9}$$

Here, $H_{1,1}$ and $H_{2,1}$ equal the actual working links in the domains. For instance, in Fig. 2(b), we have $H_{1,1} = 2$, since there are two working links, i.e., $1 \to 5$ and $5 \to 3$ in Domain 1.

Scenario 2: One domain has a restorable link failure, while the working links in the other domain are all available. To obtain the probability for this scenario to happen precisely, we remove the links on the p-cycle in a domain that are traversed by the working links protected by the other domain, assume they are always available, and merge the two end nodes of each of them into a supernode.

For instance, in Fig. 2(a), if we want to estimate the availability of lightpath $1 \to 5 \to 3 \to 6$ under the condition when Link $3 \to 6$ fails, we have to ensure that the common link of the two domains, i.e., Link $3 \to 5$, will not be considered repeatedly in both domains. Therefore, we remove Link $3 \to 5$ from Domain 2, merge Nodes 3 and 5 into a supernode, and modify the domains as in Fig. 2(c). By taking these steps, we make sure that each link is considered only once in the service availability estimation. In other words, the modified domains become truly independent.

Then, for each domain, we can calculate its availability $A_{i,2}^{(d)}$ after the aforementioned changes with the procedures in Subsection II.A using Eqs. (1)–(8). The probability for this scenario to happen is obtained as

$$A_2 = \rho^{H_{2,2}}(A_{1,2}^{(d)} - \rho^{H_{1,2}}) + \rho^{H_{1,2}}(A_{2,2}^{(d)} - \rho^{H_{2,2}}). \tag{10}$$

Scenario 3: Each domain has a link failure, but both failures can be restored independently. To obtain the probability for this scenario to happen precisely, we remove the common links from both domains and assume they are always available. Then, if the common link is an on-cycle link in the domain, we merge its two end nodes into a supernode. Otherwise, we just remove it from the topology of the domain. For instance, in Fig. 2(d), Links $3 \to 5$ and $5 \to 3$ are removed from Domains 1 and 2, while Nodes 3 and 5 are merged into a supernode in Domain 2. The rationale behind these procedures is that we assume a link failure on a common link can affect both domains and make the lightpath's service become unavailable. Note that this assumption is valid for most of the cases, but there are some very special cases in which it is invalid; for instance, when the failed common link is the straddling link of both domains, they indeed can each restore a working link failure simultaneously. Hence, we can underestimate the service availability slightly due to this assumption. For each domain, we can calculate its availability $A_{i,3}^{(d)}$ after the topology changes with the procedures in Subsection II.A using Eqs. (1)–(8). The probability for this scenario to happen is obtained as

$$A_3 = (A_{1,3}^{(d)} - \rho^{H_{1,3}})(A_{2,3}^{(d)} - \rho^{H_{2,3}})\rho^{L_c}. \tag{11}$$

Finally, since Scenarios 1–3 are independent, we can obtain the service availability of the dual-p-cycle case as

$$A = A_1 + A_2 + A_3. \tag{12}$$

C. Multiple-p-Cycles Case

More generally, a lightpath can be protected by multiple p-cycles. We leverage the analysis in Subsections II.A and II.B and design an iterative approach to calculate the lightpath's service availability for this case. Again, we define a protection domain as a p-cycle together with the links it protects. Then, since the lightpath is protected by multiple domains, we obtain Domains $1, 2, \ldots, n$ and the iterative approach is as follows.

Step 1: We select two domains that have common links and denote them as Domains 1 and 2, and the availability of their combination can be calculated with the procedures in Subsection II.B using Eqs. (9)–(12). Note that, when calculating the availability for Scenario 3 in Subsection II.B, the links in Domains 1 and 2 that belong to other domains are also removed to minimize inaccuracy. We denote the obtained availability as A_c:

$$A_c = \rho^{H_{1,1}+H_{2,1}} + \rho^{H_{2,2}}(A_{1,2}^{(d)} - \rho^{H_{1,2}}) + \rho^{H_{1,2}}(A_{2,2}^{(d)} - \rho^{H_{2,2}})$$
$$(A_{1,3}^{(d)} - \rho^{H_{1,3}})(A_{2,3}^{(d)} - \rho^{H_{2,3}})\rho^{L_c}. \tag{13}$$

Step 2: We merge Domains 1 and 2 into a new Domain 1, select a new Domain 2 from the unprocessed domains, update the parameters for the new Domains 1 and 2, and calculate the availability of their combination with the procedures in Subsection II.B using Eqs. (9)–(12).

Step 3: We repeat Steps 1 and 2 until all domains are merged together, and then A_c is the service availability of the multiple-p-cycle case.

D. Numerical Simulations

In this subsection, we design simulations to verify the aforementioned theoretical analysis on service availability in networks with p-cycles, and compare the results with those obtained by the method in [23,24]. Figure 3 shows the 14-node NSFNET topology that we use in the simulations. For the 14 nodes in the topology, we try all the combinations and obtain 91 source–destination (s–d) pairs. For each of the s–d pairs, we set up the routing path with shortest-path routing, and construct/allocate enough p-cycles to protect each link along the path. Note that we precalculate all 518 unidirectional cycles in the NSFNET topology, of which each will not traverse one node more than once, using the method in [25]. Then, we allocate them as the links' p-cycles with a protection efficiency (PE)-based p-cycle selection algorithm [25].

In the simulations, our failure model assumes that the link failures appear independently on each link in the topology following a Poisson process with an arrival rate of λ,

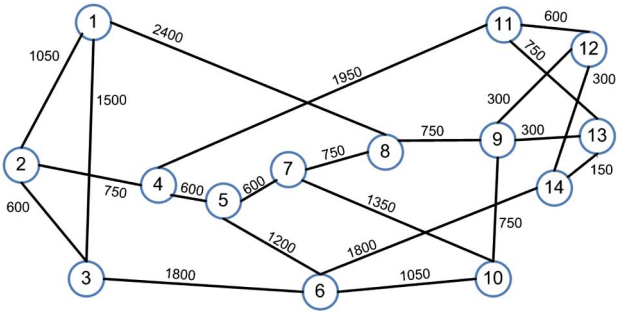

Fig. 3. Fourteen-node NSFNET network topology (fiber lengths in kilometers).

TABLE I
SERVICE AVAILABILITIES OF LIGHTPATHS IN NSFNET ($\rho = 0.99$)

Lightpath $s\leftrightarrow d$	Simulation	Our Model	Reference Model in [24]	Deviation of Our Model	Deviation of Reference Model
5↔13	0.998944	0.998914	0.999000	−3.01E−5	5.56E−5
1↔14	0.998744	0.998720	0.998800	−2.33E−5	5.64E−5
3↔12	0.998932	0.998918	0.999000	−1.38E−5	6.80E−5
4↔8	0.998889	0.998829	0.999100	−5.99E−5	2.11E−4
1↔2	0.999810	0.999801	0.999800	−9.00E−6	1.00E−5
6↔9	0.999409	0.999407	0.999400	−1.68E−6	−8.70E−6
10↔11	0.999239	0.999209	0.999300	−2.97E−5	6.12E−5
2↔5	0.999321	0.999312	0.999400	−9.18E−6	7.89E−5
6↔11	0.999115	0.999114	0.999200	−1.08E−6	8.49E−5
10↔14	0.999138	0.999117	0.999400	−2.16E−5	2.62E−4
1↔6	0.999431	0.999408	0.999400	−2.35E−5	−3.15E−5
8↔13	0.999417	0.999406	0.999400	−1.09E−5	−1.70E−5
Average of All	**0.999246**	**0.999219**	**0.999308**	**−2.75E−5**	**6.16E−5**

and their repair durations obey a negative exponential distribution with a mean of μ [26,27]. Hence, the link availability can be calculated as

$$\rho = 1 - \frac{\mu}{\frac{1}{\lambda}} = 1 - \mu \cdot \lambda. \tag{14}$$

We first set the link availability as $\rho = 0.99$, with $\mu = 10$ time units and $\lambda = 0.001$ link-failure/time-unit, and numerically calculate the service availabilities of the lightpaths between all the s–d pairs. Table I summarizes both the numerical and theoretical results. Note that, to obtain each numerical result in Table I, we simulate 2×10^7 events to ensure sufficient statistical accuracy. Since the results for all 91 lightpaths follow a similar trend, we include only the results for 12 lightpaths in Table I and show the average values. Compared with the numerical results, the theoretical results obtained by our model achieve smaller deviations than those from the reference model. On average, our model can reduce the deviation by 3.41E−5. We also observe that our model always underestimates the service availability slightly, while the reference model provides overestimated results in most cases. Note that, for service availability, underestimation is usually preferred over overestimation in network operation, since, for the network operators, overestimation on service availability may result in a higher risk of violating the SLAs and can consequently cause a bigger revenue loss.

We then run the same simulations with $\rho = 0.999$, and similar results are obtained. For all 91 lightpaths, the average service availability from the simulations, our model, and the reference model are 0.9999923, 0.9999921, and 0.9999931, respectively, and on average, our model reduces the deviation by 4.26E−7. The aforementioned numerical results are obtained by simulating 2×10^8 events for sufficient statistical accuracy. We also perform the simulations with a 24-node US backbone topology, as shown in Fig. 4 with $\rho = 0.99$. Here, we still simulate 2×10^7 events for each data point. The average deviation of the reference model is 5.74E−5, while our model provides an average deviation of −4.55E−5. Therefore, we can see that our model achieves more accurate estimations in all simulation scenarios.

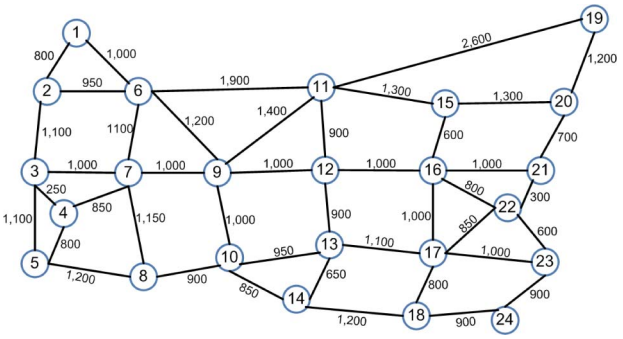

Fig. 4. Twenty-four-node US Backbone network topology (fiber lengths in kilometers).

III. SERVICE AVAILABILITY ORIENTED p-CYCLE PROTECTION DESIGN IN EONS

In this section, we design service availability oriented p-cycle design algorithms for dynamic EONs based on the theoretical analysis in Section II. Basically, we would like to 1) develop p-cycle design algorithms to protect lightpaths in EONs against any single link failures, and 2) consider service availability in the design process such that the service availability of each provisioned lightpath can be improved.

For a given EON, the topology is modeled as a graph $G(V, E)$, where V is the node set and E represents the set of directed links. The lightpath request can be denoted as $LR(s, d, n)$, where $s, d \in V$ are the source and destination nodes and n is the bandwidth requirement in terms of the number of contiguous FSs. The lightpath requests arrive and expire dynamically. For each request $LR(s, d, n)$, we need to set up its working path $s \to d$, and then configure p-cycles for all the links along the working path to protect the lightpath against any single link failures. In addition to these, we also consider the lightpath's service availability and try to maximize it during the provisioning. We assume that there are no spectrum converters in the EON, and hence, the spectrum assignments of the working path and the corresponding p-cycles have to be identical, according to the working principle of p-cycle. In this work, we

assume that different lightpaths can share the same backup resources on a p-cycle as long as they do not have common links on the p-cycle.

We first study how a lightpath's service availability is related to the working path and the p-cycles that protect it. Different from our previous analysis in Section II, which enumerates all the link-failure scenarios in which the lightpath can still be restored, we perform an approximation here. Basically, we ignore the situations in which there is more than one failed working link, but the lightpath can still be restored, since their possibilities contain terms with high order of $1-\rho$ and make only very small contributions to the total availability. By doing this, we can simplify the calculation of service availability. Note that, as our purpose here is to study what the components are that a lightpath's service availability is mainly related to and to design the algorithm accordingly, this is a reasonable approximation. After the approximation, we need to consider only two scenarios for calculating the availability:

- all the working links are working, or
- only one of the working links fails and it can be restored.

Therefore, we obtain the approximated service availability as

$$A \approx \rho^H + \sum_{i=1}^{H} (1-\rho)\rho^{H-1}\rho^{L_i}(\rho^{L_{c,i}} + 0.5L_{c,i}(1-\rho)\rho^{L_{c,i}-1}), \quad (15)$$

where L_i denotes the number of p-cycle links that are used to protect working link i, and $L_{c,i}$ represents the number of working links that can compete for backup resources with working link i. Note that we have $\rho^{L_{c,i}} + 0.5L_{c,i}(1-\rho)\rho^{L_{c,i}-1} \approx \rho^{0.5L_{c,i}}$ when $\rho \to 1$ (as shown in Fig. 5 for $\rho = 0.99$), and then Eq. (15) can be reduced to

$$A \approx \rho^H + \sum_{i=1}^{H} (1-\rho)\rho^{H-1}\rho^{L_i + 0.5L_{c,i}}. \quad (16)$$

From Eq. (16) we can see that, when the working path is determined, the lightpath's service availability is related to the term $L_i + 0.5L_{c,i}$ of each working link.

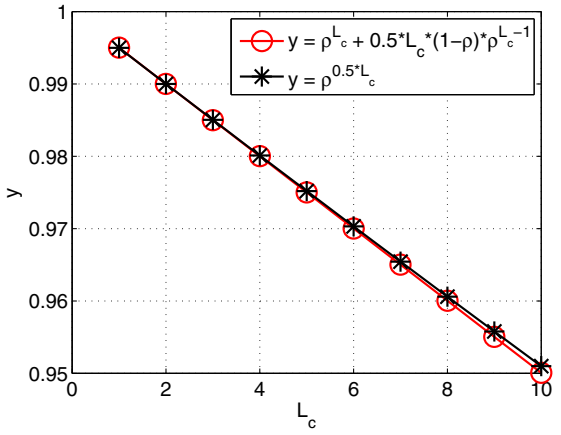

Fig. 5. Curve fitting for $\rho^{L_{c,i}} + 0.5L_{c,i}(1-\rho)\rho^{L_{c,i}-1} \approx \rho^{0.5L_{c,i}}$ with $\rho = 0.99$.

Definition [Number of relevant links (NRL)]. For a working link i, we define its NRL as $L_i + 0.5L_{c,i}$, where L_i is the number of p-cycle links that are used to protect it, and $L_{c,i}$ represents the number of other working links that can compete for backup resources with it.

Apparently, according to Eq. (16), the smaller a working link's NRL, the larger its availability. Therefore, we design a NRL-based p-cycle configuration algorithm (NRL-p-cycle) as shown in Algorithm 1. Lines 1 and 2 are for pre-computation, and basically, for the given topology $G(V,E)$, we pre-calculate a large set of cycles and store them in the cycle set $\mathbb{C}$. In Lines 4–6, we collect a dynamic request $LR(s,d,n)$ and obtain its working path with shortest-path routing. In Lines 8–20, we perform NRL based p-cycle configuration to protect all the links in the working path $\mathcal{R}_{s,d}$. Line 9 finds all the cycles in $\mathbb{C}$ that can protect one or more working links in $\mathcal{R}_{s,d}$. Then, for each of the selected cycles, we calculate the NRL for the working link that it protects, and if the cycle can protect more than one working link in $\mathcal{R}_{s,d}$, the average NRL for all of them is calculated. Then, we treat this value as the NRL of the cycle and try to configure p-cycles for all the working links by selecting cycles in ascending order of their NRLs, as shown in Lines 10–19. In Lines 21–27, we try to find the common available FSs on $\mathcal{R}_{s,d}$ and the configured p-cycles, and assign n contiguous FS′ among them using first-fit to provision the request. The reason that we assign FSs only among the common available FS′ on $\mathcal{R}_{s,d}$ and the configured p-cycles is that we assume that there are no spectrum converters in the EON, and hence, the spectrum assignments of the working path and the corresponding p-cycles have to be identical.

Algorithm 1 NRL-Based p-Cycle Configuration Algorithm

```
1  pre-calculate a large set of cycles in G(V,E);
2  store the cycles in ℂ;
3  while network is operational do
4      collect an incoming request LR(s,d,n);
5      release resources of the expired requests;
6      calculate the shortest path as the working path R_{s,d};
7      if there are not enough FSs on R_{s,d} for LR(s,d,n)
       then
8          mark LR(s,d,n) as blocked;
9          continue;
10     end
11     while there are unprotected links on R_{s,d} do
12         flag = FALSE;
13         find all the cycles in ℂ that can protect one or more
           working links in R_{s,d};
14         for each cycle in ascending order of their NRLs
15         do
15             if there are enough FSs on the cycle then
16                 mark the corresponding working link(s)
                   as protected;
17                 flag = TRUE;
18             break;
19         end
20     end
21     if flag = FALSE then
22         mark LR(s,d,n) as blocked;
23         break;
```

```
    end
  end
  if the request is not blocked then
    find the common available FSs on R_{s,d} and the
    selected cycles;
    allocate n contiguous FSs;
    if the common available FSs do not contain n
    contiguous FSs then
      mark LR(s,d,n) as blocked;
    end
  end
end
```

Definition [Protection efficiency (PE)]. If a p-cycle $\mathcal{C}$ can protect m links simultaneously in the working path $\mathcal{R}_{s,d}$, its PE is

$$\eta = \frac{m}{|\mathcal{C}|}, \tag{17}$$

where $|\mathcal{C}|$ returns the number of links in $\mathcal{C}$.

In addition to NRL-p-cycle, we also design two benchmark algorithms based on the PE of p-cycles. The first benchmark algorithm, PE-p-cycle, has similar procedures as Algorithm 1, but we replace NRL with PE and make it select p-cycles in descending order of their PEs. It is also known that a p-cycle with a smaller number of hops usually provides higher service availability [3]. Based on this idea, we design the second benchmark algorithm, PE-p-cycle-Constrained, which has exactly the same procedures as PE-p-cycle, but we restrict the largest number of hops of the candidate cycles to a fixed value and remove longer candidate cycles in $\mathbb{C}$.

IV. Performance Evaluation

In this section, we evaluate the performance of the algorithms. We use the NSFNET topology in Fig. 3 and set the link availability $\rho = 0.99$. For the EON, we assume that each FS has a bandwidth of 12.5 GHz and each fiber link accommodates 358 FSs. We apply a uniform traffic model where the source and destination nodes of each request are randomly chosen. The dynamic requests arrive according to a Poisson process, while their service periods follow the negative exponential distribution. The bandwidth requirement of each request is evenly distributed within the FSs [3,10]. For PE-p-cycle-Constrained, we restrict the largest number of hops of the candidate cycles in $\mathbb{C}$ below 7.

Figure 6 shows the results on average service availability of the lightpaths for different traffic loads. Note that we estimate the service availability of each lightpath using the analysis model developed in Section II. It can be seen that, among the three algorithms, NRL-p-cycle always achieves the highest lightpath service availability. PE-p-cycle-Constrained provides higher lightpath service availabilities than PE-p-cycle, and when the traffic load increases, the benefit from limiting the length of the candidate cycles gets amplified. This is because, for a higher traffic load, it is more likely for PE-p-cycle to select long p-cycles, which can potentially decrease the lightpath's availability. This analysis can be verified with the results on average number of hops per configured p-cycle in Fig. 7. We observe that NRL-p-cycle uses the shortest p-cycles among the three algorithms, while for PE-p-cycle and PE-p-cycle-Constrained, their difference on the average number of

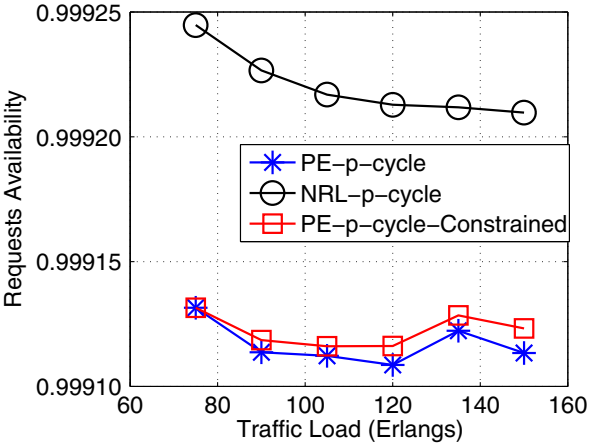

Fig. 6. Simulation results on lightpath service availability.

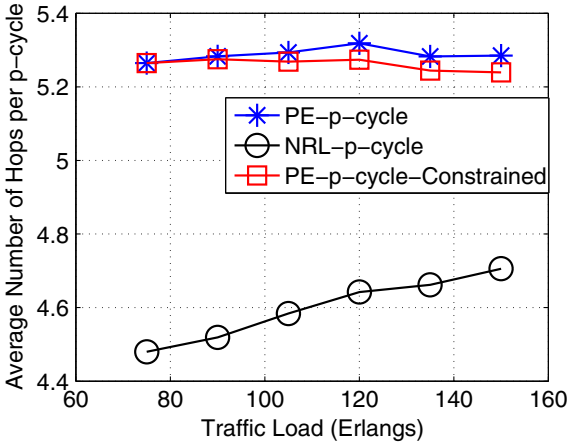

Fig. 7. Simulation results on average number of hops per p-cycle.

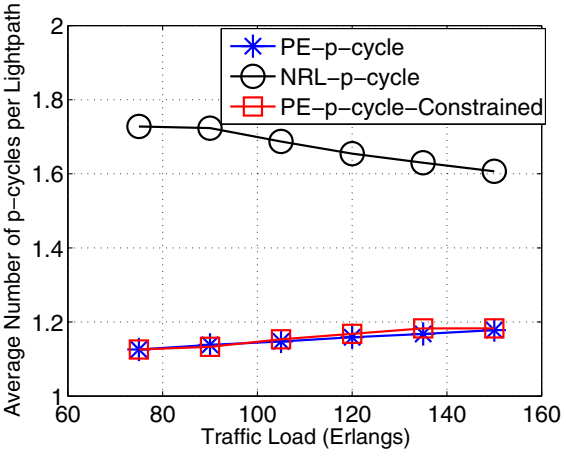

Fig. 8. Simulation results on average number of p-cycles per lightpath.

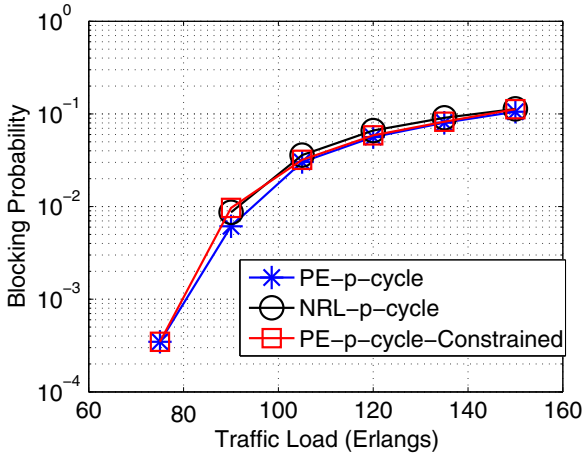

Fig. 9. Simulation results on blocking probability.

hops per p-cycle becomes larger when the traffic load increases. Figure 8 shows the average number of p-cycles configured for each lightpath. We observe that NRL-p-cycle configures the most p-cycles per lightpath for obtaining high service availability. Finally, Fig. 9 illustrates the results on blocking probability and it can be seen that the three algorithms provide almost the same blocking performance.

V. Conclusion

In this paper, we first developed a theoretical model to precisely analyze the service availability of networks with p-cycles. By considering the dependence among protection domains and all the scenarios when a lightpath is available, our model can estimate the service availability more precisely than those in previous work. Then, based on the availability analysis, we proposed a service availability oriented p-cycle configuration algorithm for dynamic EONs. The simulations compared the proposed algorithm with two benchmark p-cycle design algorithms that were based on the protection efficiency of p-cycles. Simulation results indicate that the proposed algorithm can effectively improve the service availability in EONs while keeping the blocking probability almost unchanged.

Acknowledgments

This work was supported in part by the Program for New Century Excellent Talents in University (NCET) under Project NCET-11-0884, the National Natural Science Foundation of China (NSFC) under Project 61371117, the Fundamental Research Funds for the Central Universities (WK2100060010), and the Strategic Priority Research Program of the Chinese Academy of Sciences (XDA06010301).

References

[1] O. Gerstel, M. Jinno, A. Lord, and B. Yoo, "Elastic optical networking: a new dawn for the optical layer?" *IEEE Commun. Mag.*, vol. 50, no. 2, pp. S12–S20, Apr. 2012.

[2] J. Cai, C. Davidson, H. Zhang, D. Foursa, D. Sinkin, W. Patterson, A. Philipetskii, G. Mohs, and N. Bergano, "20 Tbit/s transmission over 6860 km with sub-Nyquist channel spacing," *J. Lightwave Technol.*, vol. 30, pp. 651–657, Feb. 2012.

[3] M. Clouqueur and W. Grover, "Availability analysis of span-restorable mesh networks," *IEEE J. Sel. Areas Commun.*, vol. 20, pp. 810–821, Apr. 2002.

[4] I. Rados, P. Turalija, and T. Sunaric, "Availability model of bidirectional line switched ring," in *Proc. ICTON*, June 2001, pp. 312–316.

[5] Y. Sone, A. Watanabe, W. Imajuku, Y. Tsukishima, B. Kozicki, H. Takara, and M. Jinno, "Bandwidth squeezed restoration in spectrum-sliced elastic optical path networks (SLICE)," *J. Opt. Commun. Netw.*, vol. 3, pp. 223–233, Mar. 2011.

[6] S. Xu, Y. Yeo, Z. Xu, X. Cheng, and L. Zhou, "Shared-path protection in OFDM-based optical networks with elastic bandwidth allocation," in *Proc. of OFC*, Mar. 2012, pp. 1–3.

[7] A. Castro, L. Velasco, M. Ruiz, and J. Comellas, "Single-path provisioning with multi-path recovery in flexgrid optical networks," in *Proc. of ICUMT*, Oct. 2012, pp. 745–751.

[8] M. Klinkowski and K. Walkowiak, "Offline RSA algorithms for elastic optical networks with dedicated path protection consideration," in *Proc. of ICUMT*, Oct. 2012, pp. 670–676.

[9] A. Eira, J. Pedro, and J. Pires, "Spectrum and transponder optimization in survivable translucent flexible-grid optical networks," in *Proc. of ICC*, June 2012, pp. 6235–6240.

[10] X. Cai, K. Wen, R. Proietti, Y. Yin, D. Geisler, R. Scott, C. Qin, L. Paraschis, O. Gerstel, and B. Yoo, "Experimental demonstration of adaptive combinational QoT degradation restoration in elastic optical networks," *J. Lightwave Technol.*, vol. 31, pp. 664–671, Feb. 2013.

[11] M. Liu, M. Tornatore, and B. Mukherjee, "Survivable traffic grooming in elastic optical networks—shared protection," *J. Lightwave Technol.*, vol. 31, pp. 903–909, Mar. 2013.

[12] L. Ruan and N. Xiao, "Survivable multipath routing and spectrum allocation in OFDM-based flexible optical networks," *J. Opt. Commun. Netw.*, vol. 5, pp. 172–182, Mar. 2013.

[13] S. Ramamurthy, L. Sahasrabuddhe, and B. Mukherjee, "Survivable WDM mesh networks," *J. Lightwave Technol.*, vol. 21, pp. 870–883, Apr. 2003.

[14] W. Grover and D. Stamatelakis, "Cycle-oriented distributed preconfiguration: ring-like speed with mesh-like capacity for self-planning network restoration," in *Proc. of ICC*, June 1998, pp. 537–543.

[15] D. Schupke, C. Gruber, and A. Autenrieth, "Optimal configuration of p-cycles in WDM networks," in *Proc. of ICC*, June 2002, pp. 2761–2765.

[16] H. Huang and J. Copeland, "A series of Hamiltonian cycle-based solutions to provide simple and scalable mesh optical network resilience," *IEEE Commun. Mag.*, vol. 40, no. 11, pp. 46–51, Nov. 2002.

[17] Z. Zhang, W. Zhong, and B. Mukherjee, "A heuristic method for design of survivable WDM networks with p-cycles," *IEEE Commun. Lett.*, vol. 8, pp. 467–469, July 2004.

[18] Z. Zhang, W. Zhong, and S. Bose, "Dynamically survivable WDM network design with p-cycle-based PWCE," *IEEE Commun. Lett.*, vol. 9, pp. 756–758, Aug. 2005.

[19] A. Eshoul and H. Mouftah, "Survivability approaches using p-cycles in WDM mesh networks under static traffic," *IEEE/ACM Trans. Netw.*, vol. 17, pp. 671–683, Apr. 2009.

[20] F. Ji, X. Chen, W. Lu, J. Rodrigues, and Z. Zhu, "Dynamic *p*-cycle protection in spectrum-sliced elastic optical networks," *J. Lightwave Technol.*, vol. 32, pp. 1190–1199, Mar. 2014.

[21] M. Clouqueur and W. Grover, "Availability analysis and enhanced availability design in *p*-cycle-based networks," *Photon. Netw. Commun.*, vol. 10, pp. 55–71, Jan. 2005.

[22] D. Mukherjee, C. Assi, and A. Agarwal, "An alternative approach for enhanced availability analysis and design methods in *p*-cycle-based networks," *IEEE J. Sel. Areas Commun.*, vol. 24, pp. 23–34, Dec. 2006.

[23] M. Kiaei, A. Ranjbar, C. Rocha, B. Jaumard, and C. Assi, "Improved availability models for *p*-cycle-based network design," in *Proc. of DRCN*, Oct. 2009, pp. 62–69.

[24] M. Kiaei, A. Ranjbar, B. Jaumard, and C. Assi, "An improved analysis for availability-aware provisioning in *p*-cycle-based mesh networks," *J. Lightwave Technol.*, vol. 27, pp. 4424–4434, Oct. 2009.

[25] X. Chen, F. Ji, Y. Wu, and Z. Zhu, "Energy-efficient resilience in translucent optical networks with mixed regenerator placement," *J. Opt. Commun. Netw.*, vol. 5, pp. 741–750, May 2013.

[26] R. Clemente, M. Bartoli, M. Bossi, G. D'Orazio, and G. Cosmo, "Risk management in availability SLA," in *Proc. of DRCN*, Oct. 2005, pp. 411–418.

[27] P. Cholda, A. Mykkeltveit, B. Helvik, and A. Jajszczyk, "Continuity-based resilient communication," in *Proc. of DRCN*, Oct. 2009, pp. 335–342.